Onsala Space Observatory – IVS Analysis Center Activities During 2017–2018

Rüdiger Haas, Thomas Hobiger, Hans-Georg Scherneck, Niko Kareinen, Grzegorz Klopotek, Periklis-Konstantinos Diamantidis, Joakim Strandberg

Abstract This report briefly summarizes the activities of the IVS Analysis Center at the Onsala Space Observatory during 2017–2018 and gives examples of results of ongoing work.

1 General information

We concentrate on research topics that are relevant for space geodesy and geosciences. These research topics are related to data observed with geodetic VLBI and complementary techniques.

2 Activities during the Past Two Years

We worked primarily on the following topics:

- Optimizing VLBI Intensive schedules
- Extension of the c5++ analysis software
- VLBI observing GNSS signals
- Analysis of VLBI observations of an artificial radio source on the Moon
- Distributed VLBI correlation
- Deformation of radio telescopes
- Coastal sea level observations with GNSS
- Ocean tide loading

Chalmers University of Technology, Department of Space, Earth and Environment, Onsala Space Observatory, SE-439 92 Onsala

Onsala Analysis Center

IVS 2017+2018 Biennial Report

3 Optimizing VLBI Intensive Schedules

In recent years a number of new VLBI stations for VGOS (VLBI Global Observing System) have been installed. This opens up possibilities to add new stations to the so-called IVS Intensive (INT) sessions. The currently observed INT sessions include primarily long east-west oriented baselines so that UT1-UTC can be derived from short observation sessions (one to two hours) on a daily basis. Using simulations for a complete year of INT observations, we studied the impact of adding a third station in tag-along mode to the INT

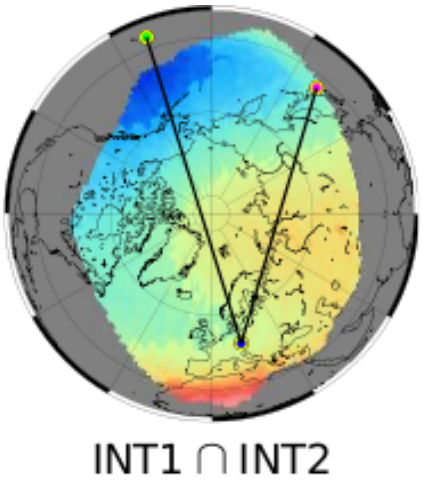

Fig. 1 Ratio of UT1–UTC weighted root-mean-square values obtained with adding a third tag-along station compared to the corresponding single-baseline session. The map is a combination referring to both IVS INT series, INT1 and INT2, with the corresponding baselines indicated. The color scale covers 0.6 (dark blue) to 0.9 (red), i.e., adding a tag-along station always gives an improvement. The largest improvement is found for stations at the Pacific coast of North America. The figure is taken from [1].

sessions [1]. The impact on the accuracy of the derived UT1–UTC is primarily controlled by a) geometry and b) atmospheric turbulence. We found that we can identify areas where the addition of a third station in tag-along mode improves the UT1–UTC estimates by up to 60%, compared to the results from the original single-baseline observations, see Figure 1. In these areas there are several upcoming VGOS sites as well as currently operational legacy S/X VLBI stations. Thus, it is easily possible to improve the performance of the IVS products for UT1–UTC.

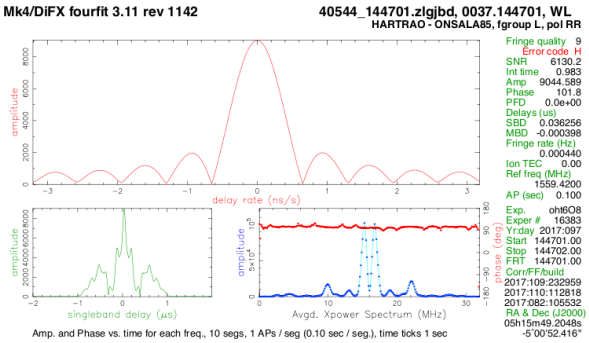

Fig. 2 Upper half of a fringe plot for a 1 s long observation of Galileo satellite PE26 on the baseline Onsala–Hartebeesthoek. Clearly, the BOC signal of Galileo is visible in the cross-power spectrum. Even with just 1 s of data, SNR $>$ 6000 is achieved.

4 Extension of the c5++ Analysis Software

The c5++ analysis software package [2] is able to perform combined data analysis of VLBI, GNSS, and SLR on the observation level. During the last two years we have been working on extending the software.

One addition is that support for the analysis of VLBI observations to near-field radio sources was included [3]. Now it is possible to a) create so-called ".im-files" for the correlation of near-field targets with DiFX, as well as b) analyzing VLBI observations of near-field targets such as, e.g., GNSS satellites (see Section 5) or the Chinese lunar lander (see Section 6), including the estimation of corresponding parameters.

Another extension concerns the analysis strategy in c5++, which so far has been based on the least-squares approach. To improve the possibilities of handling stochastic processes and to improve the combination of large data sets, an analysis strategy based on a Kalman Filter has been implemented. This allows, e.g., analysis of a complete 15 day long CONT campaign in one step while combining VLBI and GNSS on the observation level and avoiding discontinuities at day boundaries.

5 VLBI Observing GNSS Signals

We continued our efforts concerning VLBI observations of GNSS signals [4]. Several new observing sessions were performed, involving intercontinental baselines and observations of signals of GPS and GLONASS as well as Galileo. We streamlined our data processing and analysis, which is now done with DiFX, Fourfit, and c5++. As an example of the post-correlation analysis, a fringe plot using 1 s of data observed on the baseline Onsala–Hartebeesthoek for Galileo satellite PE26 is presented in Figure 2. This shows that scan lengths as short as 1 s are sufficient to reach more than sufficient an SNR.

Data analysis was done with c5++, which had been extended for analysis of observations of near-field targets (see Section 4). Because the observations were performed at one L-band frequency only, ionospheric corrections were applied based on global TEC maps provided by the IGS. However, these are neither accurate nor detailed enough; thus, additional station-dependent ionospheric biases were estimated. A priori

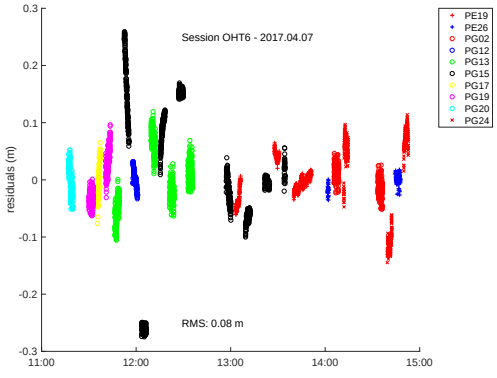

Fig. 3 Post-fit residuals of the analysis of session OHT6 (Hartebeesthoek–Onsala) on 7 April 2017. Several GPS (PGxx) and Galileo satellites (PExx) were observed, see legend. The RMS of the residuals is 8 cm.

tropospheric information was used based on the GPT2 model, and corrections in the form of zenith wet delays (ZWD) were estimated. To account for further instrumental effects, also satellite-specific time biases were estimated. Using this approach, post-fit residuals on the order of less than 10 cm can be achieved. As an example, the post-fit residuals for the observing session OHT6 are presented in Figure 3.

6 Analysis of VLBI Observations of an Artificial Radio Source on the Moon

A lot of work has been spent on the so-called OCEL (Observations of the Chang'E Lander) sessions. There are twelve OCEL sessions that were observed from 2014 to 2016 with global networks of VLBI stations, see [5]. A Monte Carlo simulation study [6] based on the actual OCEL schedules showed that under perfect conditions it should be possible to achieve a 2D position precision of about 10 cm on the Moon's surface, see Figure 4.

In a follow-up simulation study [7] we investigated whether observations of the lunar lander could be included in regular IVS R1-sessions using a scan-replacement strategy. Again, extensive Monte Carlo simulations were performed which led to the result that such a strategy appears feasible and could result in a 2D position accuracy on the order of better than 0.5 m, assuming the same lunar observation precision as before. Performing a corresponding simulation study and including lunar lander observations in VGOS schedules, the expected 2D accuracy could even be as good as 5 cm.

The analysis of real data of two of the OCEL sessions resulted in horizontal position uncertainties on the lunar surface of 8.9 m and 4.5 m in latitude and longitude [8].

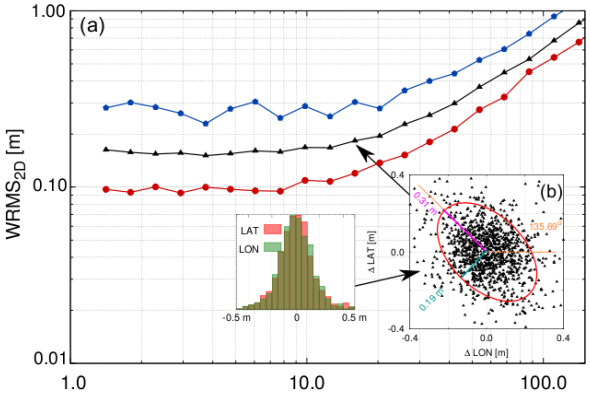

Fig. 4 (a) Performance of OCEL sessions for the 2D position accuracy of the lunar lander, as a function of assumed measurement precision of lunar observations. The mean performance based on all twelve OCEL sessions is depicted in black, while the results of the best and the worst performing sessions are depicted in red and blue, respectively. (b) Scatter plot and histograms of the lander's 2D position solutions from Monte Carlo simulations based on all OCEL sessions and assuming a lunar observation precision of 15.97 mm. The error ellipse represents the 1-σ confidence level. The figure is taken from [6].

7 Distributed Correlation

We participated in an IVS Pilot Project on distributed correlation [9]. Several hours of data of two R1 sessions were distributed to a number of "branch correlators", among them Onsala. Each branch correlator received one (individual) hour of data from all stations involved in the R1 sessions. These data were correlated at the branch-correlators with DiFX and the corresponding output files were sent to the central correlator at MPIfR in Bonn. The Bonn correlator followed two approaches: a) correlating all data, including post-correlation analysis and creation of databases, and b) using the data correlated at the branch correlators for the post-correlation analysis and creation of another set of databases. The comparison between these two approaches showed that there are no significant differences detectable. The pilot project should be continued with further sessions, also including VGOS observations. However, these first results show that distributed correlation can become an interesting approach for the upcoming VGOS era where huge amounts of data will be collected and need to be correlated. Distributed correlation could reduce the load of individual correlation centers.

8 Geometry of Radio Telescopes

During the last two years, the geometry of the radio telescopes at Onsala was studied. This includes both the gravitational deformation of the 20-m radio tele-

scope [10], as well as the investigation of the surface accuracy of the new Onsala twin telescopes [11].

9 Scheduling of Twin Telescopes

With three VGOS twin telescopes becoming operational, an important question is how to use them in an optimal way. The VLBI scheduling software packages need to be extended accordingly by implementing corresponding scheduling rules. Using the example of the Onsala twin telescopes, different scheduling approaches were tested. Schedules were prepared with four different approaches, forcing the telescopes to either 1) observe the same source, 2) observe in orthogonal directions, 3) observe in opposite azimuth but identical elevation directions, or 4) observe in random directions. Additionally, different radio source distributions were tested: square-root or uniformly distributed. Using Monte Carlo simulations, observations were generated based on these schedules. The simulated data were analyzed in a simplified point-positioning strategy, and station positions and tropospheric parameters were estimated and compared to the a priori used (true) simulation parameters. Preliminary results are presented in Figure 5 and show that, compared to the same source approach, all alternative scheduling approaches give improved results for station positions and zenith wet delays. While the performance is rather identical for station positions, there appears to be an advantage concerning ZWD when forcing the telescopes to observe in opposite directions.

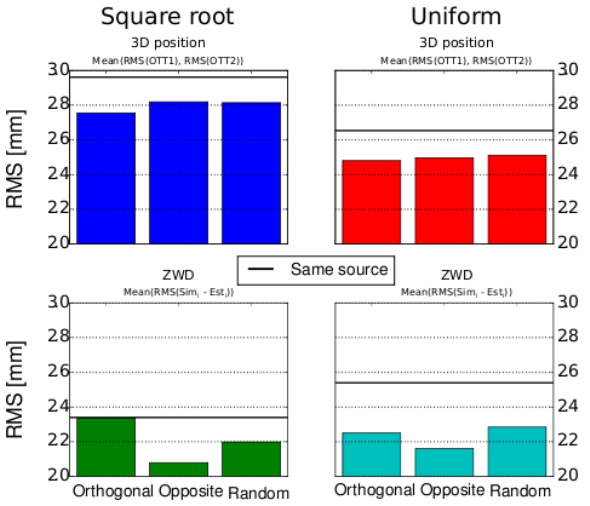

Fig. 5 Root mean square (RMS) comparisons of results for station position and zenith wet delay (ZWD) for different scheduling approaches for twin telescopes. The figure is taken from [12].

10 Coastal GNSS Reflectometry

We continued our research in the field of GNSS reflectometry. The analysis strategy was extended to successfully allow the detection of sea ice [13]. Furthermore, the analysis software was developed to enable real-time GNSS-R results based on Kalman filter analysis [14]. We showed that it is advantageous to use multi-GNSS signals to derive sea level with GNSS-R [15]. The standard deviation of the multi-GNSS solution (GPS+GLONASS+Galileo) for sea level, compared to a co-located traditional tide gauge, is lower than each of the individual solutions, or combinations of just two GNSS (see Figure 6).

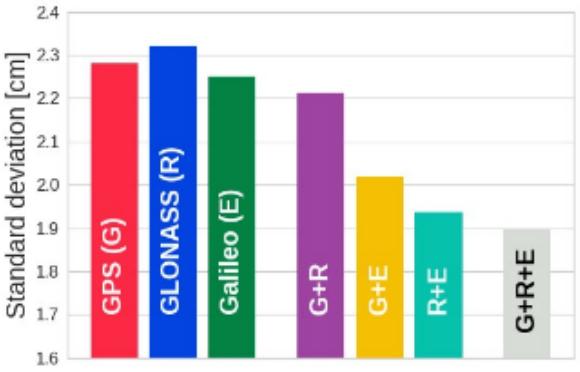

Fig. 6 Standard deviation between a traditional tide gauge and GNSS-R results for sea level. The figure is taken from [15].

11 Ocean Tide Loading

The Automatic Ocean Tide Loading service was operated throughout the year. It is heavily used by the international scientific community. Both new ocean models and new Green's functions were included during the last two years, see `http://holt.oso.chalmers.se/loading/`.

12 Future Plans

The IVS Analysis Center at the Onsala Space Observatory will continue its efforts to work on specific topics relevant to space geodesy and geosciences. We plan to intensify our work in particular concerning tropospheric parameters sensed by space geodetic techniques. The motivations are that the Onsala twin telescopes will become operational and are expected to contribute with a very interesting data set and also that a third microwave radiometer has been installed at Onsala. Thus, a special focus for the next two years is on the Onsala twin telescopes, to connect them to the legacy S/X VLBI network, and to analyze tropospheric parameters and their spatial and temporal variation. We will also continue our efforts concerning VLBI observations of GNSS signals.

References

1. Kareinen N, Klopotek G, Hobiger T, Haas R (2017). Identifying optimal tag-along station locations for improving VLBI Intensive sessions *Earth Planets Space*, 69(1), 16, doi:10.1186/s40623-017-0601-y
2. Hobiger T, Otsubo T, Sekido M, Gotoh T, Kubooka T, Takiguchi H (2010). Fully automated VLBI analysis with c5++ for ultra rapid determination of UT1. *Earth Planets Space*, 62(12), 933–937, doi:10.5047/eps.2010.11.008
3. Klopotek G, Hobiger T, Haas R (2017) Implementation of VLBI Near-Field Delay Models in the c5++ Analysis Software. In: A. Nothnagel and F. Jaron (eds.) *Proc. First Int. Workshop VLBI Obs. Near-field Targets*, 29–33
4. Haas R, Hobiger T, Klopotek G, Kareinen N, Yang J, Combrinck L, de Witt A, Nickola M (2017). VLBI With GNSS-signals on an Intercontinental Baseline – A progress report. In: R. Haas and G. Elgered (eds.), *Proc. 23rd EVGA Working Meeting*, 117–121
5. Haas R, Halsig S, Han S, Iddink A, Jaron F, La Porta L, Lovell J, Neidhardt A, Nothnagel A, Plötz C, Tang G, Zhang Z (2017). Observing the Chang'E-3 Lander with VLBI (OCEL) – Technical Setups and First Results. In: A. Nothnagel and F. Jaron (eds.) *Proc. First Int. Workshop VLBI Obs. Near-field Targets*, 41–64
6. Klopotek G, Hobiger T, Haas R (2017). Lunar Observations and Geodetic VLBI – A Simulation Study. In: R. Haas and G. Elgered (eds.), *Proc. 23rd EVGA Working Meeting*, 122–126
7. Klopotek G, Hobiger T, Haas R (2018). Geodetic VLBI with an artificial radio source on the Moon: a simulation study. *Journal of Geodesy*, 92:457–469 doi:10.1007/s00190-017-1072-4
8. Klopotek G, Hobiger T, Haas R, Jaron F, La Porta L, Nothnagel A, Zhang Z, Han S, Neidhardt A, Plötz C (2019). Position determination of the Chang'e 3 lander with geodetic VLBI. *Earth Planets Space*, 71:23, doi:10.1186/s40623-019-1001-2
9. Bertarini A, Tuccari G, Haas R, McCallum J, Weston S (2017). An IVS Pilot Study for Distributed Correlation in the VGOS era. In: R. Haas and G. Elgered (eds.), *Proc. 23rd EVGA Working Meeting*, 49–50
10. Bergstrand S, Haas R, Herbertsson M, Rieck C, Spetz J, Svantesson C-G (2017). Geometric Variations of a Geodetic Radio Telescope. In: R. Haas and G. Elgered (eds.), *Proc. 23rd EVGA Working Meeting*, 61–64
11. Lösler M, Eschelbach C, Haas R (2017). Unified Model for Surface Fitting of Radio Telescope Reflectors In: R. Haas and G. Elgered (eds.), *Proc. 23rd EVGA Working Meeting*, 29–34
12. Kareinen N (2017). Observation strategies for current and future geodetic very long baseline interferometry. PhD thesis, Chalmers University of Technology, ISBN 978-91-7597-741-6, new series nr 4422, ISSN 0346-718X
13. Strandberg J, Hobiger T, Haas R (2017) Coastal Sea Ice Detection Using Ground-Based GNSS-R. *IEEE Geoscience and Remote Sensing Letters*, 14(9), 1552–1556, doi:10.1109/LGRS.2017.2722041
14. Strandberg J, Hobiger T, Haas R (2018) Towards Real-time GNSS Reflectometry Using Kalman Filtering. *Proc. IGARSS 2018*, 2043–2046
15. Strandberg J, Hobiger T, Haas R (2018) Inverse modeling of reflected GNSS signals for measurement of the environment. *Proc. ENC 2018*, 99–100